Novel Biobased Self-Healing Ionomers Derived from Itaconic Acid Derivates

Josefine Meurer, Julian Hniopek, Jan Dahlke, Michael Schmitt, Jürgen Popp, Stefan Zechel, and Martin D. Hager*

This article presents novel biobased ionomers featuring self-healing abilities. These smart materials are synthesized from itaconic acid derivates. Large quantities of itaconic acid can be produced from diverse biomass like corn, rice, and others. This study presents a comprehensive investigation of their thermal and mechanical properties via differential scanning calorimetry (DSC), thermo gravimetric analysis (TGA), and FT-Raman and FT-IR measurements as well as dynamic mechanic analysis. Within all these measurements, different kinds of structure-property relationships could be derived from these measurements. For example, the proportion of ionic groups enormously influences the self-healing efficiency. The investigation of the self-healing abilities reveals healing efficiencies up to 99% in 2 h at 90 °C for the itaconic acid based ionomer with the lowest ionic content.

Awareness for more sustainable production and use of functional materials, in particular synthetic polymers, not only determines current world politics and public debate, but has also been a major topic in research for a long time.[1–3] The majority of the plastic manufacturing industry relies on non-renewable feedstocks for the production of plastics due to limiting factors for biobased materials such as availability, price and performance.[4] Thus, it is difficult to replace currently used materials based on non-renewable resources with more sustainable materials. One promising example for a building block for biobased polymers is itaconic acid (IA).[5–6] Amongst other synthetic pathways, it is possible to produce large quantities of IA by modern biotechnological methods with the microorganism *Aspergillus terreus*.[7] Biomass derived from corn starch, lignocellulosic feedstock as well as rice can be utilized for the fermentation process.[8–11]

However, the use of itaconic acid-based polymers poses several issues that must be considered. Polymers derived directly from itaconic acid tend to dehydrate and decarboxylate at higher temperatures.[12–13] This problem was not found for the corresponding diester species of IA. The polymerization process itself is often realized by condensation reactions leading to polyester structures.[14–17] Another method for the polymerization of IA is via ring-opening-metathesis polymerization.[17] The radical homo polymerization of IA is rather difficult due to the low reactivity and potential side reactions.[13,18] However, there are already some methods established.[19–20] Furthermore, it is possible to utilize the anhydride or esters as monomers in different radical polymerization methods.[20–23] Hereby, it is also possible to apply modern controlled radical polymerization methods such as atom-transfer radical polymerization (ATRP) or reversible addition-fragmentation chain transfer polymerization (RAFT).[24–25]

In order to design new sustainable materials and polymers, two main targets can be identified. On the one hand, the starting materials should be based on renewable resources featuring a good availability as well as accessibility via environmentally friendly and efficient production technologies. On the other hand the life-cycle and the durability of the materials has to match the desired application.[26] One option can be the use of self-healing materials to enhance the period of use of functional materials. [27–28]

Ionic interactions have been utilized in intrinsic self-healing polymers (the so-called ionomers).[29–31] These polymers contain low amounts of ionic groups within a polymer matrix
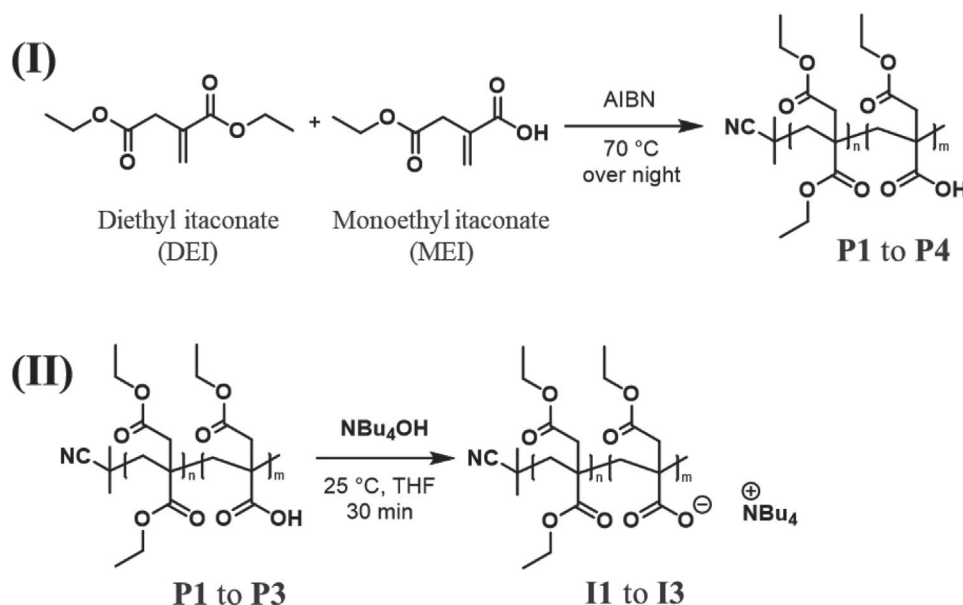
J. Meurer, Dr. Jan Dahlke, Dr. S. Zechel, Dr. M. D. Hager
Laboratory of Organic and Macromolecular Chemistry (IOMC)
Friedrich Schiller University Jena
Humboldtstr. 10, Jena 07743, Germany
E-mail: martin.hager@uni-jena.de
J. Meurer, Dr. Jan Dahlke, Dr. S. Zechel, Prof. J. Popp, Dr. M. D. Hager
Jena Center for Soft Matter (JCSM)
Friedrich Schiller University Jena
Philosophenweg 7, Jena 07743, Germany
J. Hniopek, Prof. M. Schmitt, Prof. J. Popp
Institute of Physical Chemistry (IPC)
Friedrich Schiller University Jena
Helmholzweg 4, Jena 07743, Germany
J. Hniopek, Prof. M. Schmitt, Prof. J. Popp
Abbe Center of Photonics (ACP)
Friedrich Schiller University Jena
Albert-Einstein-Straße 6, Jena 07745, Germany
J. Hniopek, Prof. J. Popp
Leibniz Institute of Photonic Technology
e. V. Jena, Albert-Einstein-Straße 9, Jena 07745, Germany

Scheme 1. Schematic representation of I) the synthesis of the polymers **P1** to **P4** via free radical polymerization of monoethyl and diethyl itaconate and II) the preparation of the ionomers **I1** to **I3** utilizing tetrabutylammonium hydroxide.

with low dielectric constant. Attractive interactions between the charged functional groups favor the formation of dynamic and thermo-reversible ionic aggregates, also known as multiplets or clusters.[32] Consequently, this type of polymer is highly suitable for the design of self-healing materials.[33–35]

In this work, we present new ionic polymers that combine the different approaches towards sustainable material design. The materials consist of mono- and diethyl itaconic acid esters, which can be derived from renewable resources, neutralized with a metal free tetrabutylammonium base.

Three different ionomers (**I1** to **I3**) were synthesized and characterized. The preparation of these ionomers was performed via a two-step synthesis (**Scheme 1**). The synthesis started with the preparation of the polymers via free radical polymerization (FRP) of 4-ethyl methylene succinate (further named as: monoethyl itaconate, MEI) and diethyl itaconate (DEI) (see Scheme 1 (**I**)). During the polymerizations, the content of the monoethyl itaconate was varied (5%, 10%, and 15%) to gain polymers with different compositions and later with different amounts of ionic groups to investigate the influence of the ionic content on the properties (detailed information regarding characterization can be found in Figure S1 and Tables S1 and S2 in the Supporting Information).

The molar masses were determined via size exclusion chromatography (SEC) and the results are summarized in **Table 1** (Figures S2 and S3, Supporting Information). It was found that all polymers show comparable molar masses and distribution. This is important to disregard the influence of factors like entanglement length and molar mass on the properties of the polymers and ionomers and to be able to focus more on the structural differences such as the ionic content. Furthermore, the composition of the polymers **P1** to **P3** was determined via titration with KOH (detailed information in the SI). The ratios found in the polymers are very close to the initially utilized ratios of the monomers for the polymerization (Table 1; Table S3, Supporting Information). As intended, it was possible to synthesize polymers with about 5 to 15% MEI.

For the synthesis of the ionomers the calculated content of MEI was utilized to determine the amount of tetra-N-butyl ammonium hydroxide required for the complete neutralization of the polymer. In order to prepare the ionomers, each polymer was dissolved in THF and the required amount of NBu_4OH was added (see Scheme 1 (**II**)). Tetra-N-butyl ammonium hydroxide cannot be produced out of renewable resources; however, it was utilized for the neutralization due to the successful application in other self-healing ionomers in the past.[36]

Table 1. Determined molar masses and distribution via SEC, compositions via titration with KOH and thermal properties via differential scanning colorimetry and thermo gravimetric analysis for the polymers **P1** to **P3**.

	Results of the size exclusion chromatography[a]			Content of MEI found via titration[b] [%]	Thermal properties[c] [°C]	
	M_n [g mol^{-1}]	M_w [g mol^{-1}]	Đ		T_g	T_d
P1	27 400	49 100	1.79	5.3	50	273
P2	36 500	64 000	1.75	10.7	53	273
P3	34 000	66 400	1.96	16.1	56	272

[a] Eluent: THF + 0.1% TFA; PMMA-standard; [b] 0.05 M KOH solution in ethanol, indicator: phenolphthalein; [c] determined temperatures for the tempered polymer samples.

2000636 (2 of 6)

Consequently, three different ionomers **I1** to **I3** were obtained. Detailed information about the synthesis and characterization of the ionomers are presented in Tables S4 and S5 in the Supporting Information.

The thermal properties, in particular the thermal stability, are important parameters for intrinsic self-healing materials. Hence, the self-healing process is often thermally triggered, the material must withstand longer periods of time at elevated temperatures (often up to 100 °C or higher). Consequently, no degradation or side-reactions should occur during the healing process.

Firstly, a thermogravimetric analysis (TGA) was performed for all polymers and the corresponding ionomers to determine the degradation temperature (T_d) (Table S2 and S5 and Figure S8 to S11, Supporting Information). The TGA revealed that the degradation occurs at lower temperatures in the ionomers compared to the polymer they are derived from. In addition, it was also found that the ionic content has an enormous influence on the degradation temperature. The polymer as well as the ionomer with the highest amount of MDI (**P3** and **I3** about 16%) showed by far the lowest degradation temperature. In contrast, for the polymer and the ionomer with the lowest content of carboxylic acid respectively carboxylate groups (about 5%) a much higher degradation temperature was determined. Starting from a temperature of about 100 °C a small, but continuous mass loss can be observed (see Figure S8 to S10). This phenomenon could indicate the occurrence of undesired temperature triggered side-reactions during the heating step. The fact, that this effect increases with the MEI content suggests that this reaction is presumably involving the carboxylic acid and the carboxylate, respectively. Therefore, all polymers and ionomers were annealed for 12 h at 130 °C and measured again. During the annealing, little bubbles were observed, which become less and less with time. The former mentioned little, but continuous mass loss in the range from 100 to 300 °C was not detectable in the measurement of the annealed polymers.

Furthermore, via differential scanning calorimetry (DSC) measurements it was possible to determine the glass transition temperatures (T_g) of **P1** to **P3** and **I1** to **I3** (Table S2 and S5, Figure S4 to S7, Supporting Information). All DSC measurements were performed with the annealed samples to avoid degradation during the DSC study. Beside this fact, the first cycle of the DSC measurement is usually used as annealing step to clear the thermal history of the sample. Furthermore, the DSC measurements revealed significant differences between the polymers and the corresponding ionomers. Interestingly, it was found that the polymers show higher values for the T_g (about 55 °C) compared to the corresponding ionomers (about 30 °C). This phenomenon may be based on the addition of the tetra-*N*-butyl ammonium hydroxide for neutralization. The tetrabutylammonium cation might act as a softener due to the long alkyl chains. Furthermore, the composition of the polymer or ionomer influences the T_g as well. The T_g of the polymers ranges from 56 °C for **P3**, the one with the highest amount of MEI, to 50 °C for the one with the lowest, **P1**. It is possible that the acid group forms hydrogen bonds with carbonyl groups in the polymer side chains leading to a supramolecular crosslinking. In contrast, the T_g decreases slightly with the amount of MEI for the ionomers, which is caused by the plasticizing cation.

Additionally, for the three ionomers a dynamic mechanic analysis (temperature sweep from 130 to 25 °C) was performed. Further information about this measurement is presented in the supporting information, the resulting graphs are shown in Figure S21. The T_g-values obtained in this measurement are slightly higher compared to the DSC measurements, but still in a similar range.

To investigate the structural changes during thermal treatment of the neutral polymers **P1** to **P3**, and the respective ionomers **I1** to **I3**, Raman- and IR-spectroscopy were performed before and after the annealing process. For **P1** to **P3** the Raman- and IR spectroscopic measurements revealed that the free acid groups of the polymers undergo dehydration to form cyclic anhydrides,[37] which can be monitored well using Raman spectroscopy (details, Scheme S1 (I), Supporting Information).

In contrast, the behavior of **I1** to **I3** is more complicated: The general structure of the Raman spectrum of **I3** remains unchanged during the annealing process, most notably no new bands arise in the spectrum. The largest changes visible in the Raman spectrum are the significant decrease of a band at 1325 cm^{-1} and a remarkable increase in the intensity of the C = O stretching vibration band around 1730 cm^{-1} (Figure S13). By comparison of the spectrum with the Raman spectra of **I3KOH** (an ionomer neutralized with KOH instead of NBu$_4$OH), tetrabutylammonium bromide as well as tributylamine, it was possible to assign the band at 1325 cm^{-1} to the C-N stretching vibration of the NBu$_4^+$ ion, indicating a loss of NBu$_4^+$ (for further information and spectra see SI). Notably it is still possible to observe a signal in this region, which proves that only parts of the NBu$_4^+$ get lost during the annealing process. Combined with the loss of NBu$_4^+$, the carbonyl vibration increases in intensity. This observation can be explained by comparing the spectra to the Raman spectrum of **I1**. Here the intensity of the C = O stretching vibration is also higher than in **I3**. Considering the higher ratio of DEI to MEI in **I1**, this shows that the carbonyl vibration increases in intensity if more ester groups are present in a polymer. This is consistent with the Raman spectra of **P4** (a DEI homopolymer, which only contains ester functionalities, see Figure S16), for which the intensity of the C = O stretching band is even higher and with the known lower activity of the C = O stretching vibrations in carboxylic acids compared to esters.[38]

IR spectroscopy provides further insight into the changes during annealing. Figure S15 shows the IR spectra for the same samples. Contrary to its very low Raman activity, which prevents its detection for the samples investigated here, the asymmetric COO$^-$ vibration of the carboxylate group shows high IR absorbance and can be detected at 1585 cm^{-1}. The intensity of this band decreases significantly during the annealing process, but, corresponding to the observed loss of NBu$_4^+$ in the Raman spectrum, not completely.

Considering this, the most likely mechanism for the changes during annealing is a partial trans-alkylation of one of the butyl chains from the quaternary ammonium ion to the carboxylate resulting in tributylamine and an ethylbutyl itaconate unit in the polymer (see Scheme S1 (II), Supporting Information).

To confirm this proposed mechanism, an IR spectrum of the gas phase over **I2** during tempering was recorded. Since IR spectroscopy is a highly sensitive method, the vapor pressure of

the tributylamine at 150 °C is sufficient to be detected in the gas phase. Indeed, the gas phase IR spectrum in large parts agrees with the IR spectrum of pure tributylamine thus supporting the proposed mechanism (see Figure S14, Supporting Information). Comparing the band areas of the residual asymmetric COO⁻ vibration of the carboxylate in the IR spectra of **I1** to **I3** after annealing (see Figure S15 and S19, Supporting Information), it is furthermore apparent that the amount of residual carboxylate depends on the amount of MEI in the original polymer. Therefore, it can be followed that a roughly constant ratio of COO^-/Bu_4N^+ is the cause for the ionomeric behavior and shows strong enough interaction as to not be reactive under the annealing conditions.

Due to the results of the Raman- and IR-spectroscopic investigation, which indicated a partly loss of the ionic groups in the ionomers during the annealing step, rheology measurements were performed. These measurements should prove the presence of ionic supramolecular crosslinking. For this reason, frequency sweeps of the ionomers were performed (detailed information in the Supporting Information, Figure S22 to S24). For reversible supramolecular networks usually, a crossover of G' and G'' is detected during a frequency sweep measurement.[] After the crossover (at higher frequencies) the behavior of the sample changes and the storage modulus (elastic properties) is dominant. For each ionomer (**I1** to **I3**) frequency sweep measurements at two different temperatures were performed. First, a measurement at 25 °C, where the supramolecular network should be in a quasi-irreversible state (temperature

low → exchange reaction extremely slowed or prevented). Second, a measurement at 90 °C was performed (above T_g and activation of the supramolecular bonds). The expected behavior could be observed for all ionomers. At 25 °C the storage modulus lies nearly one decade above the loss modulus indicating a kind of permanent crosslinking. At 90 °C the former described behavior of supramolecular crosslinked networks could be observed. The crossover of G' and G'' was detected at a frequency of about 10 Hz for all ionomers, which corresponds to a supramolecular bond life time of 0.08 s.

To investigate the self-healing abilities in a comparable manner, an established experimental setup and evaluation procedure based on tactile measurements was applied.[35,39] The healing efficiency (H_eff) could be calculated based on the volume of the initial scratch (V_I) compared to the volume after certain healing steps (V_H) (Equation 1).

$$H_{eff} = 100\% \left(1 - \frac{V_H}{V_I} \right) \qquad (1)$$

For this reason, samples of the annealed ionomers were prepared (detailed information in the SI). The surface was damaged with an indenter followed by a profile measurement of the initial scratch. Exemplarily, the picture of the scratch and the corresponding 3D-profile for the ionomer **I1** is shown in **Figure 1** (left side). Afterwards, the sample was annealed for 2 h at 90 °C to trigger the healing process. Subsequently, the area of the scratch was investigated optically (photo) and via a profile
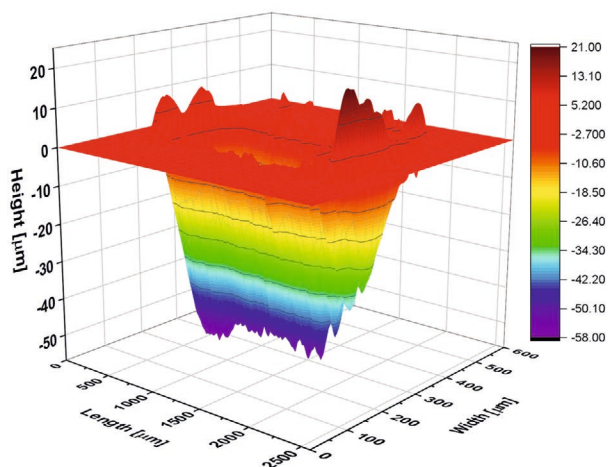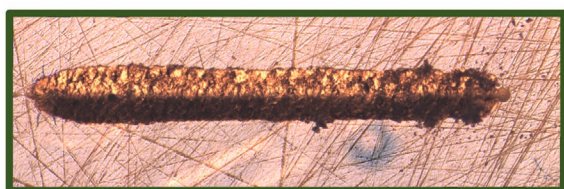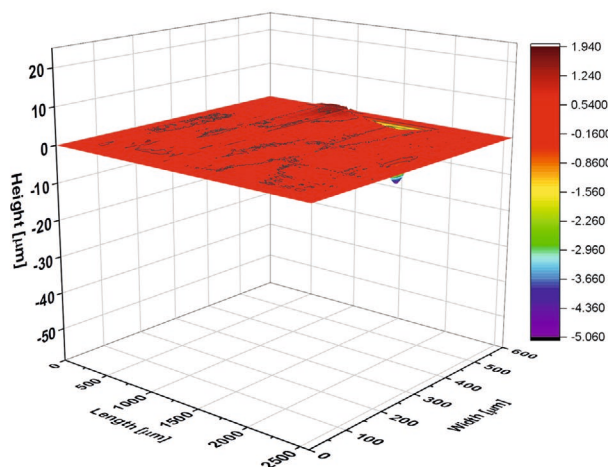
Figure 1. Optical images (top) and 3D-plot of the profile measurement (bottom) of the ionomer **I1** during the performed scratch-healing test (left: Surface with scratch; right: Surface after healing for 2 h at 90 °C).

measurement (see Figure 1, right side). All photos and 3D-profiles are presented in the supporting information Figure S21 to Figure S22. The calculated volumes and healing efficiencies are summarized in Table S6.

During this test **I1** (about 5% MEI) showed the best healing performance. The first healing step (2 h at 90 °C) already lead to a healing efficiency of 99.3%. Furthermore, the ionomer containing about 10% ionic moieties showed a healing efficiency above 90% after 2 h at 90 °C. Since such high values already had been determined for these two samples, no second healing step was performed. In opposite to this, the ionomer with the highest ionic content (**I3**) exhibited the worst healing performance. After the first healing step, the sample **I3** just reached a healing efficiency of 46.9%. Therefore, a second healing step was carried out with this sample (same conditions), increasing the healing efficiency to 58.1%. Consequently, an influence of the ionic content on the healing properties can be observed. Thus, increasing the ionic content leads to decreased healing ability of the ionomer. We suppose that the increased supramolecular interaction leads to a decreased mobility in the ionomer and within this a decrease of the self-healing abilities. For the ionomers **I1** and **I2**, which showed the best healing performance, the test was repeated to prove the reproducibility. The second test of the healing efficiencies revealed also efficiencies above 90%.

Furthermore, the hardness was investigated via a Vickers hardness test. Self-healing materials can be useful in almost every area where materials get damaged. Such properties are helpful to increase the lifetime of materials. One very important application of self-healing polymers is for example the use as coating. Within this field the hardness of material plays an important role. A good way to determine the hardness of material is the Vickers hardness test. The test was performed analog to literature,[35] for the annealed polymer and ionomers. A summary and comparison of the calculated values for the Vickers hardness is presented in Figure S28. During this test the calculated Vickers hardness showed for all polymers significantly higher values compared to the ionomers. As mentioned before, this effect may result from hydrogen bonds in the polymers and the softener effect of the alkyl chains in the counter ions of the ionomers. In general, the hardness decreases with the content of MEI.

It was found that the polymers are all much harder compared to the ionomers. The results are summarized in the supporting information Table S7, Figure S27 and S28.

This work presents the synthesis of novel smart polymers. One of their special features is the biobased nature combined with smart properties like self-healing behavior. The polymers are synthesized from diethyl itaconate and 4-ethyl methylene succinate. The three synthesized polymers differ in their composition (MEI content from 5 to 15%). Ionomers are formed via the neutralization reaction with tetra-*N*-butyl ammonium hydroxide. Investigation of their thermal properties via differential scanning calorimetry, thermogravimetric analysis, dynamic mechanical analysis and FT-Raman and -IR spectroscopy revealed a composition dependent degradation behavior. Furthermore, detailed self-healing tests were performed. The ionomer with the best healing behavior was able to heal 99% of the damage within 2 h at 90 °C.

Experimental Section

Detailed information about the synthesis and characterization of the polymers and ionomer are provided in the supporting information.

Supporting Information

Supporting Information is available from the Wiley Online Library or from the author.

Conflict of Interest

The authors declare no conflict of interest.

[1] S. A. Miller, *ACS Macro Lett.* **2013**, 2,550.
[2] D. K. Schneiderman, M. A. Hillmyer, *Macromolecules* **2017**, *50*, 3733.
[3] Y. Zhu, C. Romain, C. K. Williams, *Nature* **2016**, *540*, 354.
[4] X. Zhang, M. Fevre, G. O. Jones, R. M. Waymouth, *Chem. Rev.* **2018**, *118*, 839.
[5] Y. Bai, J. H. Clark, T. J. Farmer, I. D. V. Ingram, M. North, *Polym. Chem.* **2017**, *8*, 3074.
[6] R. Ouhichi, S. Pérocheau Arnaud, A. Bougarech, S. Abid, M. Abid, T. Robert, *Appl. Sci.* **2020**, *10*, 2163.
[7] M. Okabe, D. Lies, S. Kanamasa, E. Y. Park, *Appl. Microbio. Biotech.* **2009**, *84*, 597.
[8] J. T. Trotta, A. Watts, A. R. Wong, A. M. LaPointe, M. A. Hillmyer, B. P. Fors, *ACS Sustain. Chem. Eng.* **2019**, *7*, 2691.
[9] K. Yahiro, S. Shibata, S.-R. Jia, Y. Park, M. Okabe, *J. Ferment. Bioeng.* **1997**, *84*, 375.
[10] B. E. Teleky, D. C. Vodnar, *Polymers* **2019**, *11*, 1035.
[11] T. Willke, K. D. Vorlop, *Appl. Microbiol. Biotechnol.* **2001**, *56*, 289.
[12] S. Chakraborty, L. Ju, A. A. Galuska, R. B. Moore, S. R. Turner, *J. Appl. Polym. Sci.* **2018**, *135*, 46417.
[13] D. Stawski, S. Połowiński, *Polimers* **2005**, *50*,118.
[14] T. Robert, S. Friebel, *Green Chem.* **2016**, *18*, 2922.
[15] S. Brännström, E. Malmström, M. Johansson, *J. Coat. Technol. Res.* **2017**, *14*, 851.
[16] T. J. Farmer, R. L. Castle, J. H. Clark, D. J. Macquarrie, *Int. J. Mol. Sci.* **2015**, *16*, 14912.
[17] M. Winkler, T. M. Lacerda, F. Mack, M. A. R. Meier, *Macromolecules* **2015**, *48*, 1398.

[18] C. S. Marvel, T. H. Shepherd, *J. Org. Chem.* **1959**, *24*, 599.

[19] T. C. Castle, R. L. Finch, D. A. Pears, B. D. Young, A61K 8/81 (20060101); A61Q 5/06 (20060101); A61Q 1/10 (20060101); C08F 22/02 (20060101); A61Q 19/00 (20060101); ed., **2016**.

[20] B. E. Tate, in *Fortschritte der Hochpolymeren-Forschung* (Ed.: J. H. Winter), Springer Berlin Heidelberg, Berlin, Heidelberg **1967**, pp. 214.

[21] P. Sarkar, A. K. Bhowmick, *ACS Sustain. Chem. Eng.* **2016**, *4*, 2129.

[22] T. Otsu, K. Yamagishi, A. Matsumoto, M. Yoshioka, H. Watanabe, *Macromolecules* **1993**, *26*, 3026.

[23] K. Mielczarek, M. Łabanowska, M. Kurdziel, R. Konefał, H. Beneš, S. Bujok, G. Kowalski, S. Bednarz, *Macromol. Rapid Commun.* **2020**, *41*, 1900611.

[24] Z. Szablan, A. A. Toy, A. Terrenoire, T. P. Davis, M. H. Stenzel, A. H. E. Muller, C. Barner-Kowollik, *J. Polym. Sci. A: Polym. Chem.* **2006**, *44*, 3692.

[25] M. Fernández-García, M. Fernández-Sanz, J. L. de la Fuente, E. L. Madruga, *Macromol. Chem. Phys.* **2001**, *202*, 1213.

[26] C. Helbig, C. Kolotzek, A. Thorenz, A. Reller, A. Tuma, M. Schafnitzel, S. Krohns, *Sustain. Mater. Technol.* **2017**, *12*, 1.

[27] J. Dahlke, S. Zechel, M. D. Hager, U. S. Schubert, *Adv. Mater. Interfaces* **2018**, *5*, 1800051.

[28] N. van Dijk, S. van der Zwaag, *Adv. Mater. Inter.* **2018**, *5*, 1800226.

[29] J. Dahlke, R. Tepper, R. Geitner, S. Zechel, J. Vitz, R. Kampes, J. Popp, M. D. Hager, U. S. Schubert, *Polym. Chem.* **2018**, *9*, 2193.

[30] S. J. Kalista, J. R. Pflug, R. J. Varley, *Polym. Chem.* **2013**, *4*, 4910.

[31] M. Suckow, A. Mordvinkin, M. Roy, N. K. Singha, G. Heinrich, B. Voit, K. Saalwächter, F. Böhme, *Macromolecules* **2018**, *51*, 468.

[32] A. Eisenberg, B. Hird, R. B. Moore, *Macromolecules* **1990**, *23*, 4098.

[33] R. K. Bose, N. Hohlbein, S. J. Garcia, A. M. Schmidt, S. van der Zwaag, *Phys. Chem. Chem. Phys.* **2015**, *17*, 1697.

[34] N. Hohlbein, A. Shaaban, A. M. Schmidt, *Polymer* **2015**, *69*, 301.

[35] J. Dahlke, J. Kimmig, M. Abend, S. Zechel, J. Vitz, U. S. Schubert, M. D. Hager, *NPG Asia Mater.* **2020**, *12*, 13.

[36] J. Dahlke, R. K. Bose, S. Zechel, S. J. Garcia, S. van der Zwaag, M. D. Hager, U. S. Schubert, *Macromol. Chem. Phys.* **2017**, *218*, 1700340.

[37] B. E. Tate, *Makromol. Chem.* **1967**, *109*, 176.

[38] G. Socrates, *Infrared and Raman Characteristic Group Frequencies: Tables and Charts*, 3rd ed., **2004**.

[39] M. Abend, L. Tianis, C. Kunz, S. Zechel, S. Gräf, F. A. Müller, U. S. Schubert, M. D. Hager, *Polym. Test.* **2020**, *90*, 106699.